Available online at www.eccomasproceedia.org
Eccomas Proceedia UNCECOMP (2023) 822-835

ECCOMAS
Proceedia

UNCECOMP 2023
5th ECCOMAS Thematic Conference on
Uncertainty Quantification in Computational Science and Engineering
M. Papadrakakis, V. Papadopoulos, G. Stefanou (eds.)
Athens, Greece, 12-14 June 2023

PHYSICS INFORMED NEURAL NETWORKS TO MODEL THE HYDRO-MORPHODYNAMICS OF MANGROVE ENVIRONMENTS

Majdi Fanous[1], Alireza Daneshkhah[1], Juntao Yang[3], Jonathan M. Eden[2], Simon See[4,1], Vasile Palade[1]

[1]Centre for Computational Science & Mathematical Modelling
Coventry University, UK
e-mail: {fanousm2, ac5916, ab5839}@coventry.ac.uk

[2] Centre for Agroecology, Water and Resilience
Coventry University, UK
e-mail: ac6218@coventry.ac.uk

[3] NVIDIA AI Technology Center, NVIDIA, 8 Temasek Blvd, Singapore 038988, Singapore
e-mail: yjuntao@nvidia.com

[4] NVIDIA AI Technology Center, NVIDIA, Santa Clara, USA
e-mail: ssee@nvidia.com

Abstract. *Modelling the hydro-morphodynamics of mangrove environments is key for implementing successful protection and restoration projects in a climatically vulnerable region. Nevertheless, simulation of such dynamics is faced with computational and time constraints, given the nonlinear and complex nature of the problem, which could become a bottleneck for large-scale applications. The recent advances in machine learning, specifically, in physics-informed neural networks (PINNs), have gained much attention due to the potential to provide fast and accurate results, while preserving the binding physics laws and requiring small amounts of data in contrast to other neural networks. In this sense, such networks encode the physics equations into the neural network, and the latter must fit the noisy observed data whilst minimising the equation residual. This study investigates the application of PINNs to quantify the capacity of mangrove environments to attenuate waves and prevent erosion, and represents the first application of PINNs to model vegetation for a large-scale geographical domain with complex boundary conditions. Navier–Stokes, the broadly used mathematical equation to solve for fluid dynamics, is used as the governing equation that constrains the neural network to respect the conservation of mass, energy, and momentum. The Sundarbans, the largest mangrove forest in the world located between India and Bangladesh, is taken as a case study. The results demonstrate that the developed model is superior when compared to a numerical finite element model, in terms of time and data efficiency, yet produces equally strong overall results.*

Keywords: Climate modelling, Hydro-morphodynamic Modelling, Machine Learning, Physics-informed neural networks, Mangrove environments.

ISSN:2623-3339
Peer-review under responsibility of the organizing committee of UNCECOMP 2023.
doi: 10.7712/120223.10378.19649

1 INTRODUCTION

Climate change is leading to rising sea levels and increased coastal erosion around the world. As the Earth's temperature increases, the polar ice caps and glaciers melt, causing sea levels to rise. This poses a threat to low-lying coastal areas, as well as small islands, which are at risk of being inundated by the rising waters. In addition, the warming of the oceans is causing more intense and frequent storms, which can lead to more erosion of coastal areas.

Recent studies have shown that natural ecosystems, such as mangrove environments, are effective at attenuating waves and preventing erosion due to their complex root structure [10, 14, 5]. Such root structure generates friction, which decreases the incoming waves' energy. In addition, it helps trap the sediments thus preventing erosion. Mangrove environments have been recommended by the Inter-Governmental Panel on Climate Change (IPCC) under the ecosystem-based adaptation (EbA) to mitigate climate change impacts [8].

EbA is an important approach for addressing the impacts of sea-level rise and coastal erosion. For example, natural coastal defenses, such as mangroves and salt marshes, can help to protect against the impacts of storms and flooding. EbA can help to identify and prioritise the most effective and sustainable ways to adapt to the impacts of climate change, such as through the restoration of natural habitats or the protection of existing ones [15].

In order to implement successful EbA solutions, there is a need to develop an accurate simulator to the area of interest [13]. This helps in gaining better understanding of the dynamics of the region especially in the presence of mangrove environments. For example, an accurate model can provide accurate results for different climate change scenarios. Nonetheless, simulating such dynamics is non-trivial as it is faced by computational and time complexities [9]. This is particularly true when using the traditional numerical models such as finite difference, finite volume, or finite element methods to model large and complex regions.

One of the key advances recently in the field of machine learning is in physics-informed neural networks (PINNs), which have received considerable attention in modelling applications for providing fast and accurate results when compared to traditional numerical models [11, 7]. These models make use of the physics equations as regularisation terms and are implemented as penalty terms in the loss functions [2]. In this work, we use Navier–Stokes equations, that model the hydro-morphodynamics, in the PINNs model. The applicability and accuracy of the developed model is assessed against the simulation results obtained from the finite element model (FEM) developed for the selected case study.

This paper proposes employing PINNs in order to model the hydro-morphodynamics of mangrove environments. We take the Sundarbans, the largest mangrove forest in the world, as a case study to examine the performance of such networks in modelling the dynamics for a large domain with the complex boundary conditions. This paper is organised as follows: we discuss the motivation of using surrogate models to replace traditional numerical models in Section 2. Then, we explore PINNs, their usage, building blocks, and advantages in Section 3. In Section 4 we use the Sundarbans case study to showcase the performance of PINNs in modelling hydro-morphodynamics for the real-world scenarios. Finally, Section 5 concludes our work and provides insights into different usages of the proposed method.

2 MOTIVATION

Traditional numerical solvers' accuracy rely on the resolution of input data such as bathymetry, topography, mesh, and tidal data in the case for solving computational fluid dynamics (CFD) problems. Furthermore, the user has to have significant experience working with different pa-

rameter values such as viscosity and friction in order to improve the accuracy of the simulation.

Figure 1 shows the mesh that we developed to model the hydro-morphodynamics at the Sundarbans region. Simulating the Hydro and Morpho (sediment transport) dynamics for this large and irregular region with complex boundary conditions is computationally very expensive as it required spinning-up the hydrodynamics in order to avoid instability and inaccurate solutions when solving for the morphodynamics. In addition, solving equations such as Navier–Stokes too many times, required by the conventional approaches, such as Markov Chain Monte Carlo methods, to simulate the hydrodynamics and sediment concentration change, and Exner to calculate bed-level change, is computationally very expensive.

In our case, spinning-up the hydrodynamics took approximately 36 hours whereas modelling the morphodynamics took approximately 12 hours with a morphological acceleration factor applied to speed-up the bedlevel evolution. If the morphological acceleration factor was removed, the morphodynamics simulation would have taken around 18 days. Finally, any change in the parameters of the model would require repeating the full experiments again, thus increasing the time complexity significantly. This would make the process of conducting sensitivity analysis, uncertainty quantification and modelling different climate change scenarios extremely inefficient.

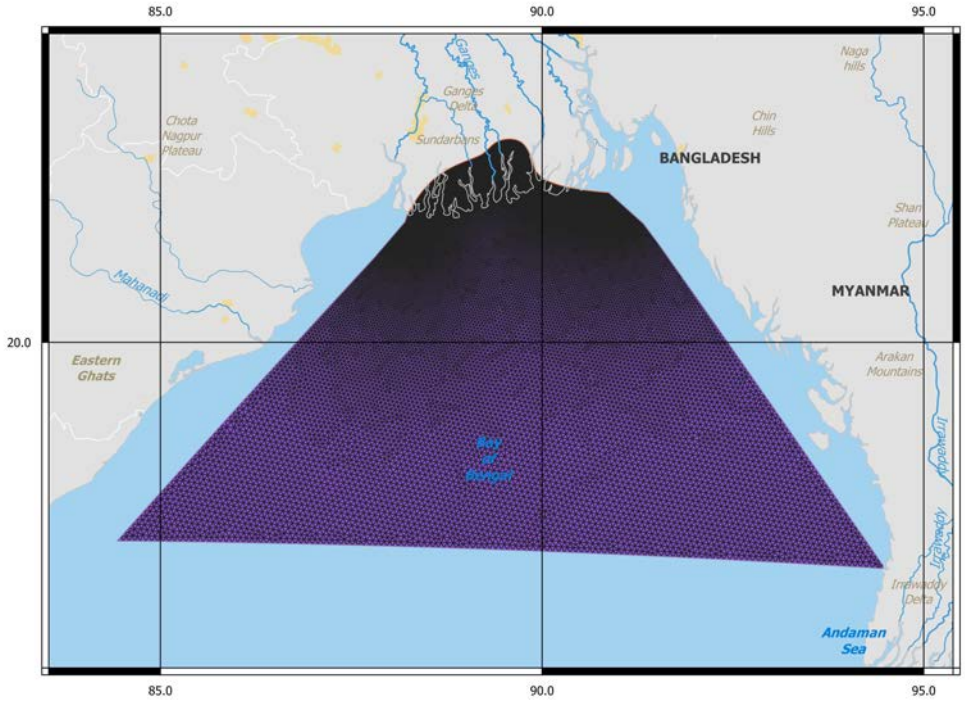

Figure 1: Mesh used to simulate the hydro-morphodynamics at the Sundarbans region. The mesh resolution varies from 1.5km at the coast to 8km deep at the sea.

Deep neural networks are fundamentally known to be able to approximate any continuous function given appropriate weights [17]. The main challenge in these networks is to properly train them by choosing the most suitable number of layers, activation function, and then training the network with enough data so that they can produce accurate outputs. Once the network is trained, predicting outputs given 'unseen' inputs is substantially fast and requires a fraction of the computational cost needed to run the numerical model as they do not need to be re-trained

[16]. This aspect of neural networks makes them suitable to replace some complex solver, such as numerical models, in a concept known as surrogate modelling. However, as stated above, the main challenge is in training these networks, and this issue arises specifically when using such networks to replace CFD solvers, since it is very expensive to run these solvers and generate large enough data, required to train the neural networks. In addition, using deep neural networks to predict the dynamics might produce physically impossible results as these are black-box models and the user has no access to the processes inside them. As a result, the output might not be reliable and could provide the results that are not accurately explainable.

PINNs have emerged as a bridge to connect governing physics laws with deep neural networks and benefit from both fields. PINNs do not require large data to train the model and can even be trained without any data [11]. PINNs would add an equation loss term to the network loss function, and then the model would tend to minimise both of these losses using Adam optimiser or LBFGS. That loss term would provide the network with a measure of the misfit, also known as residual, between the predicted gradients and the actual gradients in the differential equation which is implemented using automatic differentiation. This would ensure that the network would produce physically possible solutions by constraining the outputs of the neural network. Furthermore, once properly trained, the network would be able to provide fast predictions without the need to retrain it. We will explain the building blocks of PINNs, in Section 3, in more detail.

3 PHYSICS-INFORMED NEURAL NETWORKS

The general form of the solutions of partial differential equations (PDEs) can be expressed as

$$u_t + \mathscr{N}[u;\lambda] = 0, \mathbf{x} \in \Omega, t \in [0,T] \tag{1}$$

where $u(t,\mathbf{x})$ is the solution and $\mathscr{N}[.;\lambda]$ is a general linear or nonlinear operator with the system parameters λ. The terms t and $\mathbf{x}$ are the time and space inputs of the system, respectively. The spatial domain Ω can be bounded based on prior knowledge of the dynamical system, and $[0,T]$ is the time interval within which the system evolves. As $\mathscr{N}$ is a differential operator, one must, in general, specify the initial conditions $u(\mathbf{x},0)$ and/or the boundary conditions $u(\mathbf{x}^0,t^0)$ in order to properly define the problem and allow to solve Eq.(1).

This form encapsulates a wide range of problems where $\mathscr{N}$ can be parabolic, hyperbolic, or elliptic that model fluid dynamics, heat conduction, or steady-state diffusion, respectively.

For a two-dimensional problem, and following [11], $u(x,y,t)$ is approximated by a fully connected network $f(x,y,t)$, which takes the coordinates (x,y,t) as inputs and provides the corresponding outputs, $u_{\mathscr{N}}(x,y,t)$. The neural network is composed of multiple hidden layers, as shown in Figure 2, where each hidden neuron contains a weight $w_{i,j}$, bias b_j, and a nonlinear activation function σ such as hyperbolic tangents, ReLUs, leaky ReLUs, ELUs. or Swish[2].

We apply automatic differentiation [11] in order to determine $f(x,y,t)$ by computing the required derivatives of $u(x,y,t)$. Thus, $f(x,y,t)$ and $u(x,y,t)$ share the same parameters but with different activation functions due to the presence of the differential operation $\mathscr{N}$. The ability to apply automatic differentiation in PINNs is what makes them attractive as it is able to produce exact derivatives. As a result, there is no requirement for any form of discretisation using traditional methods such as finite differences, finite volumes, or finite element model, which eliminates the discretisation error.

The parameters of the neural network can then be learned by minimising the mean squared

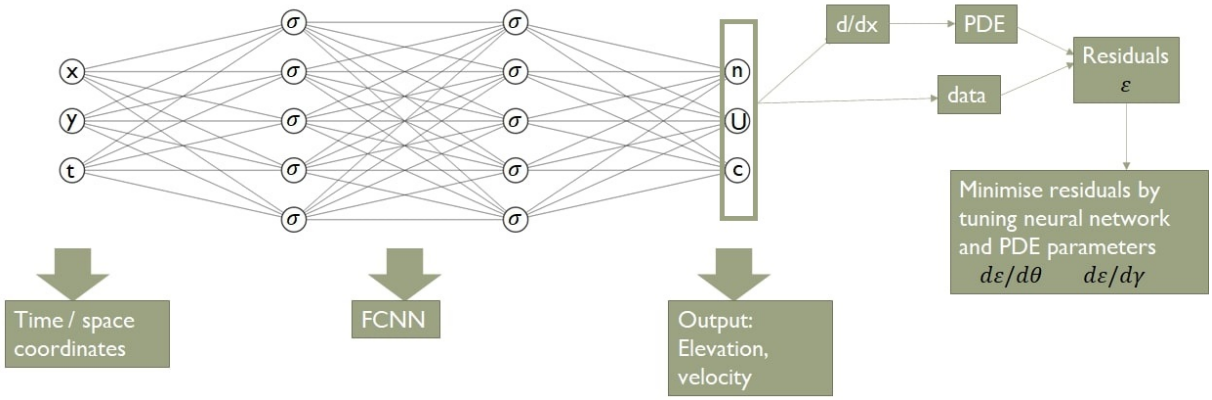

Figure 2: **Physics-informed neural network (PINN) architecture.** The inputs to the network are the time and space coordinates, which are passed through a deep fully connected neural network to obtain the desired quantities of interest such as water elevation (n), velocity (U) in both x and y directions, and sediment concentration (c). Then, gradients of the network's output with respect to its input are computed at these locations using automatic differentiation. Finally, the residual of the underlying differential equation is computed using these gradients and added as an extra term in the loss function in addition to the data loss.

error loss defined as follows

$$\mathscr{L} = \mathscr{L}_0 + \mathscr{L}_b + \mathscr{L}_r, \tag{2}$$

with

$$\begin{aligned} \mathscr{L}_0 &= \frac{1}{N_0}\sum_{i=1}^{N_0} \left\| u\left(x_i, y_i, 0\right) - I^i \right\|^2 \\ \mathscr{L}_b &= \frac{1}{N_b}\sum_{i=1}^{N_b} \left\| u\left(x_i, y_i, t_i\right) - B^i \right\|^2 \\ \mathscr{L}_r &= \frac{1}{N_r}\sum_{i=1}^{N_r} \left\| u\left(x_i, y_i, t_i\right) - r^i \right\|^2 \end{aligned} \tag{3}$$

where $\mathscr{L}_0$, $\mathscr{L}_b$, and $\mathscr{L}_r$ represent the initial loss, boundary loss, and the residuals of the governing equations, respectively; all of which are calculated on a finite set of collocation points. In addition, I^i, B^i, and r^i are the initial, boundary, and domain solutions of these collocation points respectively. Finally, the obtained residuals are minimised by tuning the neural network parameters using either a gradient descent optimiser such as Adam or L-BFGS-B, a quasi-Newton optimization algorithm [3].

4 CASE STUDY: PINNs for Modelling the Hydro-Morphodynamics of Mangroves

4.1 Governing equations

In this section, we will discuss the PDE equations used to model the hydro-morphodynamics of mangrove environments. In addition, we discuss the spatially varying parameters used to accurately model the mangrove environments in the selected case study region.

By depth-averaging from the bed, z_b, to the water surface, η, the hydrodynamic equations of the 2D model are developed. With respect to the boundary conditions, a kinematic boundary condition is applied to the water surface as a free moving boundary, where the bed is assumed to be impermeable, i.e water does not pass through the bed. Therefore, the nonlinear shallow water equations used in this model are:

$$\frac{\partial \eta}{\partial t} + \nabla \cdot (h\overline{\mathbf{u}}) = 0, \tag{4}$$

$$\frac{\partial \overline{\mathbf{u}}}{\partial t} + \overline{\mathbf{u}} \cdot \nabla \overline{\mathbf{u}} - \nu \nabla^2 \overline{\mathbf{u}} + g \nabla \eta = 0, \tag{5}$$

where $h = \eta - z_b$ is the depth, ν is the turbulent kinematic eddy viscosity, and $\overline{\mathbf{u}}$ is the depth-averaged velocity vector, where its components, $\overline{\mathbf{u_1}}$ and $\overline{\mathbf{u_2}}$, represent flow in the x and y direction, respectively (see [4] for further details).

With respect to the morphodynamics, we take a Eularian approach, which takes the concentration of sediment particles and calculates sediment dynamics using an advection-diffusion equation. Combining diffusion and dispersion effects, having a long sedimentation process, the depth-averaged sediment concentration becomes:

$$\frac{\partial}{\partial t}(\bar{c}) + \frac{\partial}{\partial x}\left(\overline{u_1 c}\right) + \frac{\partial}{\partial y}\left(\overline{u_2 c}\right) = \frac{\partial}{\partial x}\left[\left(e_s \frac{\partial \bar{c}}{\partial x}\right)\right] + \frac{\partial}{\partial y}\left[\left(e_s \frac{\partial \bar{c}}{\partial y}\right)\right] \tag{6}$$

where $\bar{c}$ is the sediment concentration, e_s is the sediment turbulent diffusivity coefficient given by $e_s = v_s^h/\sigma_s$ in which v_s^h is the horizontal viscosity and σ_s is the turbulent Schmidt number.

Since the PINNs model does not take into account any topography/bathymetry of the region, we modelled the mangrove effect at the land border by imposing a no-slip ($u_1 = u_2 = 0$) boundary condition.

Finally, to introduce tidal waves, we implemented a periodic boundary condition at the sea to introduce a tidal elevation using the following equation

$$Elevation = A \sin(2\pi t_l/T), \tag{7}$$

where A is the tidal amplitude, t_l is the simulation time, and T is the tidal period. In this model, A was chosen to be $1m$ and T is set at 12 hours, which represent a semi-diurnal tidal wave at the Bay of Bengal.

4.2 Model setup

We built our model using NVIDIA Modulus framework [1], which is a neural network framework built on top of PyTorch to develop PINNs. The developed PINNs model consists a 6 fully connected multi-layer perceptron architecture each consisting of 256 neurons that use a swish activation function. Swish is a smooth non-monotonic activation function, which performs better than ReLU on deeper models [12], and is represented by the following equation

$$\phi(x) = \frac{x}{1 + e^{-x}}. \tag{8}$$

To introduce boundary and initial conditions to PINNs, we sampled points at the boundary and the interior of the domain. *Adam* was chosen as the optimiser, and an exponential decaying learning rate of 0.95 per 100,000 iterations was selected. In addition, data obtained from Thetis, a finite element discontinuous Galerkin coastal solver [6], were used as an interior constraint to

Table 1: RMSE scores for elevation, u velocity, v velocity, and concentration at time 12, 16, 20, and 24 hours

Time (hours)	Elevation	U Velocity	V Velocity	Concentration
12	0.009	0.004	0.006	0.002
16	0.015	0.008	0.013	0.002
20	0.098	0.007	0.019	0.003
24	0.029	0.005	0.007	0.002

force the PINNs model to converge to the desired solution. Finally, an L_2 regularisation (sum of squares error) was used in order to measure the neural network's approximation error which is minimised using Adam optimiser.

We validated the performance of the neural network against Thetis at times 12, 16, 20, and 24 hours. The numerical solver was run from 30 June 1981 to 1 July 1981 and its simulation results were validated against tidal gauges records available on the above time period.

4.3 Performance metrics

In order to assess model predictive performance the Root Mean Squared Error (RMSE) of the actual, derived from the numerical model, and predicted elevation, u velocity, v velocity, and concentration at times 12, 16, 20, and 24 hours is utilised following this equation,

$$\text{RMSE} = \sqrt{E\left[(\mathbf{y} - \hat{\mathbf{y}})^2\right]}, \tag{9}$$

where $\mathbf{y}$ is the actual output taken from the numerical simulation and $\hat{\mathbf{y}}$ is the predicted output from PINNs.

4.4 Results

We trained the model over 1,000,000 iterations, using a rectangular geometry with its respective length and width being that of the Sundarbans region. The main reason of using a simplified geometry was to test the ability of PINNs to accurately predict the outputs over a tidal wave without introducing unnecessary complexities such as domain irregularities. The land border is at the bottom while the sea border is at the top of the rectangle.

To illustrate the performance of the PINNs model, Figures 3,4, 5, and 6 show the output of the PINNs model, numerical model, and the difference between both for elevation, velocity in both directions, and concentration at 4 different times of 12, 16, 20, and 24 hours. These figures show the accuracy of the PINNs model and its ability to predict different stages of the tidal wave. Another important aspect to notice in these figures is that the concentration output of the numerical model at different times was the same at about 0. This indicates the ability of mangrove environments to prevent any sediment change. Furthermore, the velocity in x direction (u) was very close to 0 in all times. This is due to the fact that the tidal wave was mostly propagating along the y-axis (i.e, from top to bottom of the rectangle) without any flow in the x direction.

Finally, the RMSE scores were calculated for the outputs at different times and are shown in Table 1. From this table, PINNs was able to overcome model variability and complexity imposed by tidal waves resulting in high accuracy predicting the outputs for a full tidal cycle.

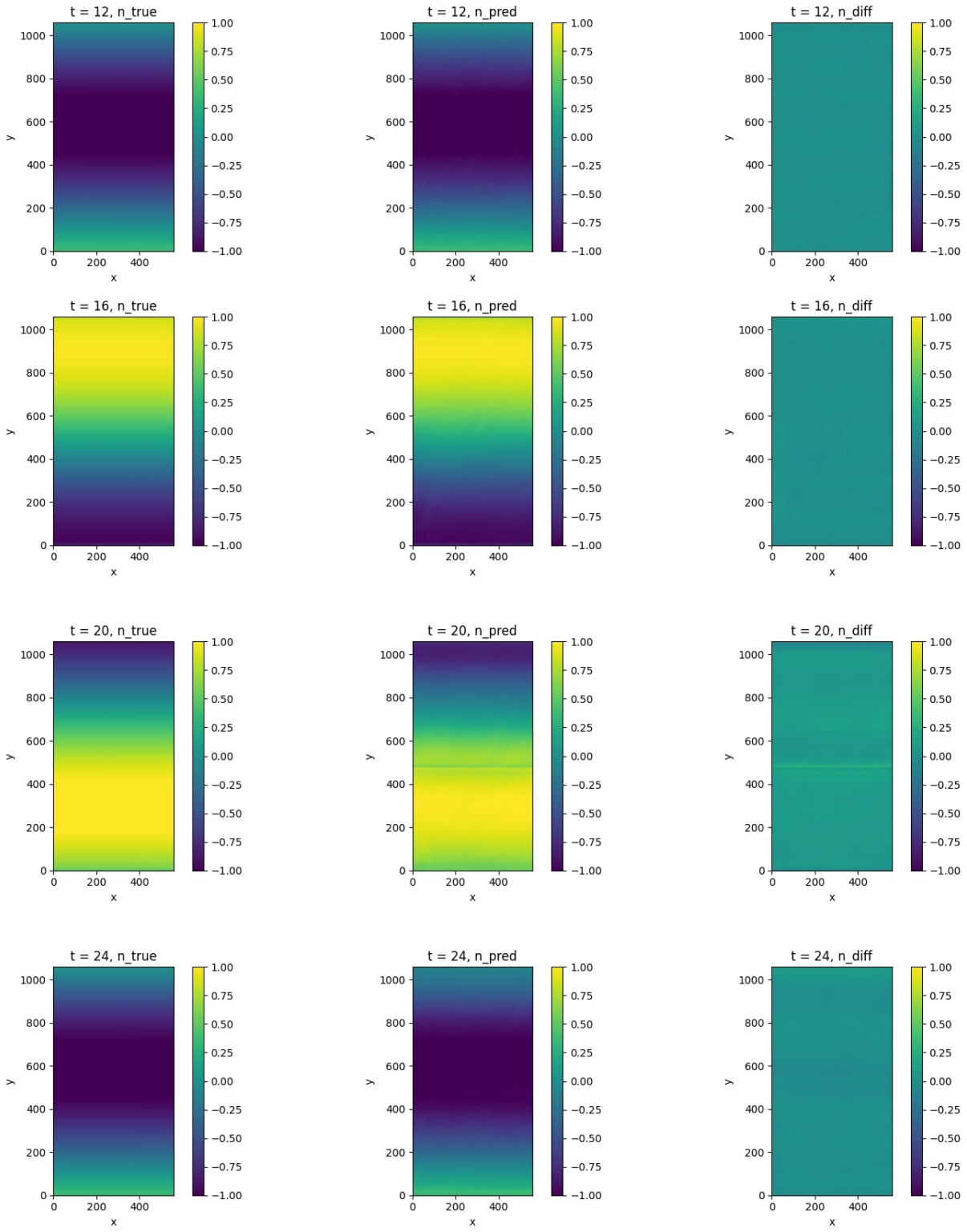

Figure 3: Actual vs predicted elevation at times 12, 16, 20, and 24 hours.

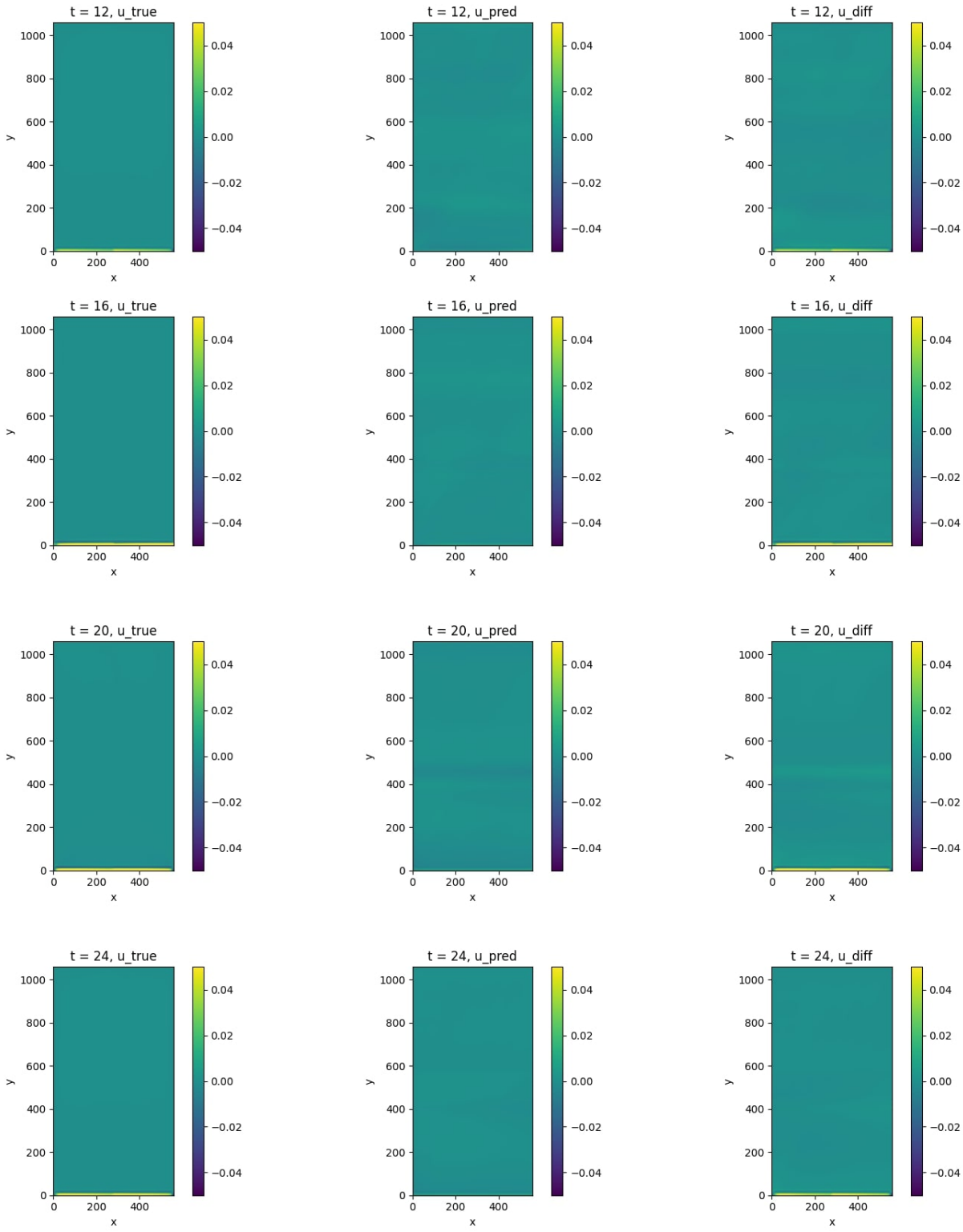

Figure 4: Actual vs predicted u velocity at times 12, 16, 20, 24 hours.

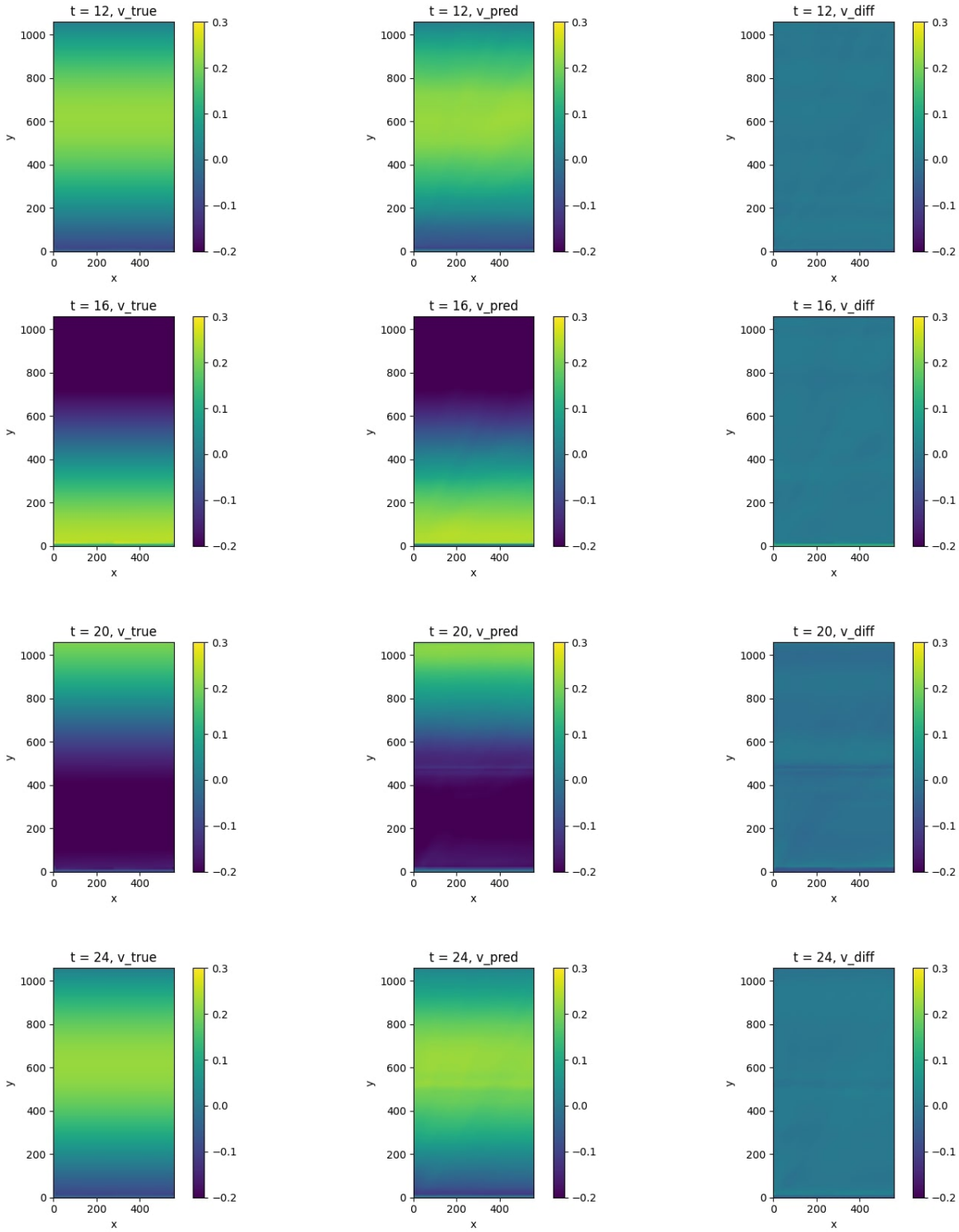

Figure 5: Actual vs predicted v velocity at times 12, 16, 20, and 24 hours.

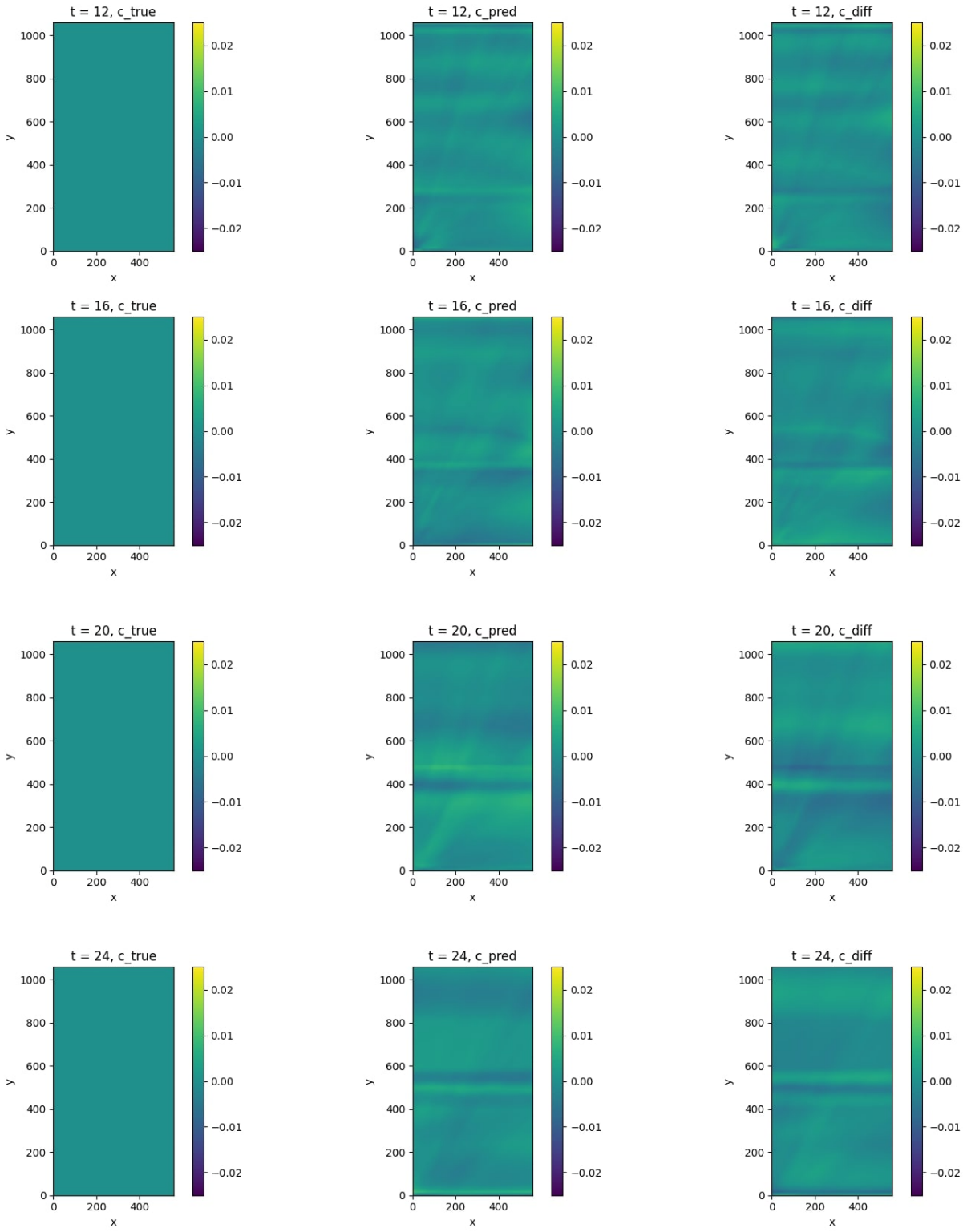

Figure 6: Actual vs predicted concentration at times 12, 16, 20, and 24 hours.

5 CONCLUSIONS

In this paper, we presented a first time application of using physics-informed neural networks to model hydro-morphodynamics around vegetation. A hybrid physics and data-driven approach was implemented to ensure the model is accurate when compared to the numerical one. Complex conditions were imposed at the model such as tidal waves and no-slip land boundary representing the effect of mangrove environments. Furthermore, the model was validated against numerical simulation data and showed close accuracy for all its outputs (elevation, velocity in x and y directions, and concentration) at different times. The model successfully predicted all outputs at different tidal wave structures showing its flexibility and ability in modelling different complexities with RMSE scores between 10^{-2} and 10^{-3}.

The major advantage of using PINNs is in inferencing where this model could predict the output for any given time in less than 10 seconds, whereas the numerical model would need to rerun the whole simulation again. Furthermore, such speed of PINNs predictions could facilitate quantifying uncertainties in the inputs and outputs of the model in a much faster performance compared to traditional numerical solvers. Another advantage of PINNs over other types of neural networks is the ability to constrain the solutions of the network to just physically realistic ones by introducing the physics equations as penalty terms in the loss function.

The results presented and conclusions drawn demonstrate the potential for the use of similar machine learning models in Earth sciences where complex dynamics are present. This method also has the capacity to improve the effectiveness of ecosystem-based adaptation solutions, to mitigate climate change impacts such as sea-level rise and land erosion, by providing fast yet accurate prediction of the region dynamics under different climate change scenarios.

6 ACKNOWLEDGEMENTS

The authors would like to thank Coventry University for funding this PhD Studentship titled “Enhancing Mangrove Forest Resilience against Coastal Degradation and Climate Change Impacts using Advanced Bayesian Machine Learning Methods”, through the GCRF Scheme.

REFERENCES

[1] Modulus — NVIDIA Developer, `https://developer.nvidia.com/modulus`

[2] Bihlo, A., Popovych, R.O.: Physics-informed neural networks for the shallow-water equations on the sphere. Journal of Computational Physics **456**, 111024 (may 2022). https://doi.org/10.1016/J.JCP.2022.111024

[3] Cuomo, S., Di Cola, V.S., Giampaolo, F., Rozza, G., Raissi, M., Piccialli, F.: Scientific Machine Learning Through Physics–Informed Neural Networks: Where we are and What’s Next. Journal of Scientific Computing 2022 92:3 **92**(3), 1–62 (jul 2022). https://doi.org/10.1007/S10915-022-01939-Z, `https://link.springer.com/article/10.1007/s10915-022-01939-z`

[4] Fanous, M., Daneshkhah, A., Eden, J.M., Remesan, R., Palade, V.: Hydro-morphodynamic Modelling of Mangroves Imposed by Tidal Waves using Finite Element Discontinuous Galerkin Method. Working Paper - Under revision at Coastal Engineering, (2023)

[5] Fanous, M., Eden, J.M., Remesan, R., Daneshkhah, A.: Challenges and Prospects of Climate Change Impact Assessment on Mangrove Environments Through Mathematical Models. Environmental Modelling and Software, (2023), https://doi.org/10.1016/j.envsoft.2023.105658

[6] Kärnä, T., Kramer, S.C., Mitchell, L., Ham, D.A., Piggott, M.D., Baptista, A.M.: Thetis coastal ocean model: Discontinuous Galerkin discretization for the three-dimensional hydrostatic equations. Geoscientific Model Development **11**(11), 4359–4382 (oct 2018). https://doi.org/10.5194/GMD-11-4359-2018

[7] Kashinath, K., Mustafa, M., Albert, A., Wu, J.L., Jiang, C., Esmaeilzadeh, S., Azizzadenesheli, K., Wang, R., Chattopadhyay, A., Singh, A., Manepalli, A., Chirila, D., Yu, R., Walters, R., White, B., Xiao, H., Tchelepi, H.A., Marcus, P., Anandkumar, A., Hassanzadeh, P., Prabhat: Physics-informed machine learning: case studies for weather and climate modelling. Philosophical Transactions of the Royal Society A **379**(2194) (apr 2021). https://doi.org/10.1098/RSTA.2020.0093, https://royalsocietypublishing.org/doi/10.1098/rsta.2020.0093

[8] Masson-Delmote, V., Zhai, P., Pirani, A., Connors, S., Pean, C., Berger, S., Caud, N., Chen, Y., Goldfarb, L., Gomis, M., Huang, M., Leitzell, K., Lonnoy, E., Matthews, J., Maycock, T., Waterfield, T., Yelekci, O., Yu, R., Zhou, B.: IPCC, 2022: Climate Change 2022: Impacts, Adaptation and Vulnerability. Contribution of Working Group II to the Sixth Assessment Report of the Intergovernmental Panel on Climate Change. Tech. rep., Cambridge University (2022)

[9] Montgomery, J.M., Bryan, K.R., Coco, G.: The role of mangroves in coastal flood protection: The importance of channelization. Continental Shelf Research **243**, 104762 (jul 2022). https://doi.org/10.1016/J.CSR.2022.104762

[10] Montgomery, J.M., Bryan, K.R., Horstman, E.M., Mullarney, J.C.: Attenuation of Tides and Surges by Mangroves: Contrasting Case Studies from New Zealand. Water 2018, Vol. 10, Page 1119 **10**(9), 1119 (aug 2018). https://doi.org/10.3390/W10091119, https://www.mdpi.com/2073-4441/10/9/1119/htmhttps://www.mdpi.com/2073-4441/10/9/1119

[11] Raissi, M., Perdikaris, P., Karniadakis, G.E.: Physics-informed neural networks: A deep learning framework for solving forward and inverse problems involving nonlinear partial differential equations. Journal of Computational Physics **378**, 686–707 (feb 2019). https://doi.org/10.1016/J.JCP.2018.10.045

[12] Ramachandran, P., Zoph, B., Le Google Brain, Q.V.: Searching for Activation Functions. 6th International Conference on Learning Representations, ICLR 2018 - Workshop Track Proceedings (oct 2017). https://doi.org/10.48550/arxiv.1710.05941, https://arxiv.org/abs/1710.05941v2

[13] Ruangpan, L., Vojinovic, Z., Di Sabatino, S., Leo, L.S., Capobianco, V., Oen, A.M., Mcclain, M.E., Lopez-Gunn, E.: Nature-based solutions for hydro-meteorological risk reduction: a state-of-the-art review of the research area. Natural Hazards and Earth System Sciences **20**(1), 243–270 (jan 2020). https://doi.org/10.5194/NHESS-20-243-2020

[14] Sánchez-Núñez, D.A., Mancera Pineda, J.E., Osorio, A.F.: From local-to global-scale control factors of wave attenuation in mangrove environments and the role of indirect mangrove wave attenuation. Estuarine, Coastal and Shelf Science **245**, 106926 (oct 2020). https://doi.org/10.1016/J.ECSS.2020.106926

[15] Seddon, N., Daniels, E., Davis, R., Chausson, A., Harris, R., Hou-Jones, X., Huq, S., Kapos, V., Mace, G.M., Rizvi, A.R., Reid, H., Roe, D., Turner, B., Wicander, S.: Global recognition of the importance of nature-based solutions to the impacts of climate change. Global Sustainability **3**, e15 (2020). https://doi.org/10.1017/SUS.2020.8

[16] Weyn, J.A., Durran, D.R., Caruana, R.: Improving Data-Driven Global Weather Prediction Using Deep Convolutional Neural Networks on a Cubed Sphere. Journal of Advances in Modeling Earth Systems **12**(9), e2020MS002109 (sep 2020). https://doi.org/10.1029/2020MS002109

[17] Zhou, D.X.: Universality of deep convolutional neural networks. Applied and Computational Harmonic Analysis **48**(2), 787–794 (mar 2020). https://doi.org/10.1016/J.ACHA.2019.06.004